

Large three-photon absorption in $\text{Ba}_{0.5}\text{Sr}_{0.5}\text{TiO}_3$ films studied using Z-scan technique

K. Venkata Saravanan,¹ K. C. James Raju,^{1,2} M. Ghanashyam Krishna,^{1,2} Surya P. Tewari,^{1,2} and S. Venugopal Rao^{1,a)}

¹Advanced Center of Research in High Energy Materials (ACRHEM), University of Hyderabad, Andhra Pradesh 500046, India

²School of Physics, University of Hyderabad, Hyderabad, Andhra Pradesh 500046, India

(Received 4 March 2010; accepted 15 May 2010; published online 10 June 2010)

Large picosecond nonlinearities in $\text{Ba}_{0.5}\text{Sr}_{0.5}\text{TiO}_3$ thin films, grown at different temperatures *in situ* on (100) MgO substrates using rf magnetron sputtering technique, were studied using the Z-scan technique. The nonlinear absorption mechanism, studied near 800 nm using ~ 2 and 25 ps pulses, switched from reverse saturable absorption type in the films deposited at temperature < 600 °C to three-photon absorption (3PA) in the films deposited at temperature > 600 °C. The magnitude of the 3PA coefficient was estimated to be $\sim 10^{-21}$ cm^3/W^2 . Two-photon absorption (2PA) was the dominant mechanism recorded with ~ 6 ns pulses. The observed behavior is correlated with morphological and crystallographic texture of the films. The linear refractive index and optical band gap of the films have also been calculated and these show a strong dependence on the substrate temperature. © 2010 American Institute of Physics. [doi:10.1063/1.3447930]

Ferroelectric thin films have significant applications in realizing several devices such as memories, tunable phase shifters, filters, oscillators, and antennas owing to its high dielectric constant, relatively low dielectric loss tangent, and large electric field tunability.^{1–4} $(\text{Ba},\text{Sr})\text{TiO}_3$ (BST) thin films possessing excellent pyroelectric and ferroelectric properties combined with stable operation at high temperatures have received particular attention in the recent years. The importance of these films, along with their doped counterparts, in nonlinear optical (NLO) applications has been established recently.^{5–18} Mishina *et al.*⁵ observed electric-field induced polarization switching of 70 nm BST films in < 55 ns, which suits the switching requirements for memory and modulator applications. Wang *et al.*⁷ observed a strong electro-optic coefficient (~ 125 pm/V) in $\text{Ba}_{0.7}\text{Sr}_{0.3}\text{TiO}_3$ thin films grown on $(\text{LaAlO}_3)_{0.3}(\text{Sr}_2\text{AlTaO}_6)_{0.35}$ substrates. However, only a small amount of effort has been embarked on to study and elucidate the optical third-order nonlinearity of epitaxial BST thin films, especially using ultrashort pulses.^{5,8–13} Herein we present our results on the NLO, optical, and physical characterization of $\text{Ba}_{0.5}\text{Sr}_{0.5}\text{TiO}_3$ films deposited on two side polished (100) MgO substrates by rf magnetron sputtering at different temperatures ranging from 500 to 800 °C. Details of the deposition procedures have been reported previously.⁴ For convenience these films are represented as BST500, BST600, BST700, and BST800 with numbers indicating the temperature during growth. Structural and morphological characterization was performed with x-ray diffraction (XRD) (Inel, CPS 120) and scanning probe microscopy (Seiko, SPA400), respectively, while the linear optical properties (refractive index and band gap) were determined from the transmittance spectra measured using a UV-Vis-near infrared spectrophotometer (JASCO, V-570). The thickness of BST500, BST600, BST700, and BST800 films, measured using a profilometer (Ambios Technology,

XP-1), were ~ 450 nm, 290 nm, 230 nm, and 210 nm, respectively.

Details and analyses of the Z-scan experiments can be found elsewhere.^{19,20} In brief, the samples were excited by laser pulses delivered by a Ti:sapphire amplifier at 800 nm, ~ 2 ps (and ~ 25 ps) pulse duration and a repetition rate of 1 kHz. The pulses were near-transform limited, which was confirmed from the time-bandwidth product. The pulses were ensured to be spatially and temporally Gaussian with the input beam diameter set to ~ 4 –5 mm. The input beam was focused using a 120 mm convex lens resulting in spot size of ~ 25 –30 μm and a Rayleigh range of ~ 3.0 –3.5 mm. The peak intensities were in the 1 – 5×10^{11} W/cm^2 range. The experiments were performed at 100 Hz.

Figure 1(a) shows open aperture Z-scan data (open circles) of BST500 recorded with ~ 25 ps pulses indicating a reverse saturable absorption (RSA) type of nonlinearity. The fit (solid line) yielded an effective nonlinear coefficient²⁰ (α_2 or β referred to as 2PA here) value of ~ 0.16 cm/GW . Inset shows the closed aperture data. A valley-peak signature indicates positive nonlinearity. The nonlinear refractive index (n_2), obtained from the fits to experimental data, increased with increasing deposition temperature (T_d) with the highest value of $\sim 3.25 \times 10^{-14}$ cm^2/W extracted for BST800 films. Figures 1(b) and 1(c) show the open aperture data for BST700 and BST800 clearly demonstrating multiphoton absorption type of behavior and best fits (solid lines) to the data yielded 3PA coefficients of $\sim 45 \times 10^{-22}$ cm^3/W^2 and $\sim 60 \times 10^{-22}$ cm^3/W^2 , respectively. Peak intensities used were $\sim 2 \times 10^{11}$ W/cm^2 for all the films. Figures 1(b) and 1(c) also demonstrate the 2PA fits (dotted lines) which were clearly off from the experimental data points in regions away from the focus. In both open and closed aperture data the contribution of substrate was insignificant. Figure 1(d) shows the open aperture data of BST500 recorded with ~ 2 ps pulses, again suggesting RSA type of behavior. The fit (solid line) yielded a 2PA coefficient value of ~ 0.16 cm/GW . Inset of Fig. 1(d) shows the closed aperture data. The signature of positive nonlinearity was intact. The nonlinear refractive

^{a)}Author to whom correspondence should be addressed. Electronic mail: svrsp@uohyd.ernet.in.

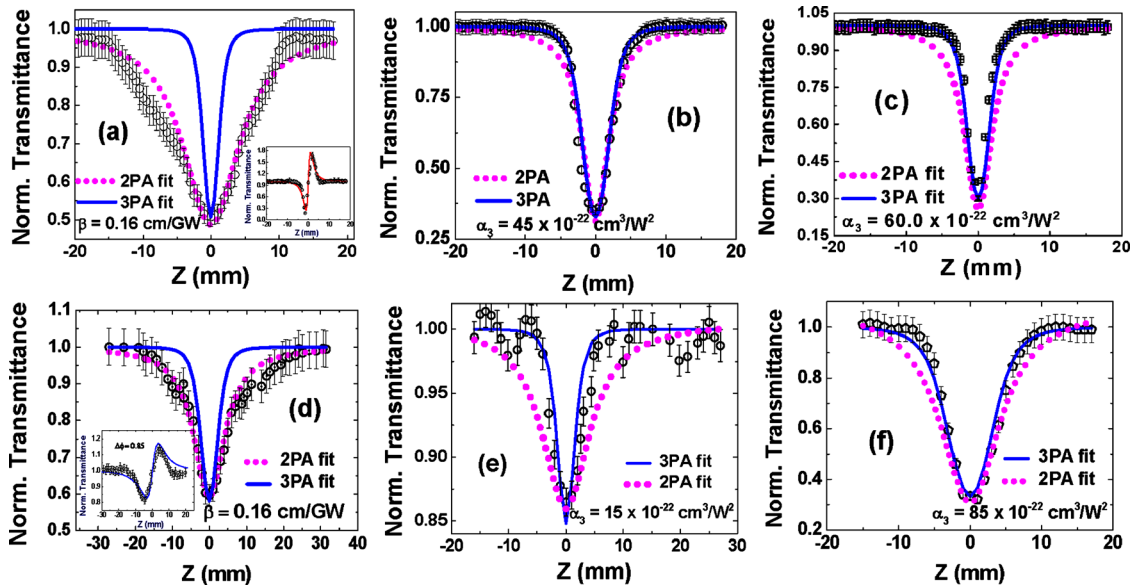


FIG. 1. (Color online) Z-scan data with ~ 25 ps pulses (a) BST500 open aperture (inset shows closed aperture data), (b) BST700 open aperture data, and (c) BST800 open aperture. Peak intensities used were 2×10^{11} W/cm 2 . Z-scan data with ~ 2 ps pulses (d) BST500 open aperture data (inset shows closed aperture data). (e) BST700 open aperture data and (f) BST800 open aperture data. Peak intensities used were $0.5\text{--}1.5 \times 10^{11}$ W/cm 2 . Solid lines are the fits for 3PA and dotted lines for 2PA.

index (n_2) once more increased with T_d with a highest value of $\sim 1.0 \times 10^{-14}$ cm 2 /W for BST800 films. Figures 1(e) and 1(f) show the open aperture data for BST700 and BST800 indicating 3PA and the fits yielded coefficients of $\sim 15 \times 10^{-22}$ cm 3 /W 2 and $\sim 85 \times 10^{-22}$ cm 3 /W 2 , respectively. Peak intensities used were $\sim 0.5\text{--}1.5 \times 10^{11}$ W/cm 2 . 2PA fits (dotted lines), which are also incorporated in the figures, were not matching with the experimental data. Figure 2 shows the open aperture data obtained with ~ 6 ns pulses at 532 nm. The fits (solid lines) provided the values of 2PA coefficient varying from 30 cm/GW for BST500 films to 110 cm/GW for BST800 films. Peak intensities used were $\sim 2 \times 10^8$ W/cm 2 . Closed aperture data did not indicate any of the peak-valley or valley-peak signatures.

Linear refractive index (n_0) and optical band gap (E_g) of the BST films were calculated using the envelope method 21 and Tauc relation, 4 respectively. The variation in n_0 (at 600

nm) and the band gap (E_g) of BST films as a function of T_d is shown in Fig. 3. The E_g of BST500 films was ~ 4.21 eV, which decreased sharply to ~ 3.83 eV for the BST600 films. The inset of Fig. 3 shows the T_d dependent XRD patterns of BST films. The films deposited at 500 $^\circ$ C and below indicated amorphous nature. The onset of crystallization was found to be 600 $^\circ$ C. Films deposited beyond 600 $^\circ$ C crystallized into cubic perovskite phase with no evidence of any secondary phase formation. The lattice constant calculated, assuming cubic crystal symmetry, was 3.949 ± 0.01 \AA , which is close to the value of 3.947 \AA , reported for bulk BST. The average crystallite size deduced using the Scherrer formula 22 was ~ 19 nm, 29 nm, and 31 nm for BST600, BST700, and BST800 films, respectively. The surface of BST500 films was smooth (rms roughness ~ 0.7 nm) with no evidence of grain growth. BST600 films had an rms roughness value of ~ 8.7 nm which decreased to ~ 3.3 nm and 2.2 nm for the films deposited at 700 $^\circ$ C and 800 $^\circ$ C, respectively. The transition in surface morphology is in good agreement with that predicted by Yang *et al.* 23

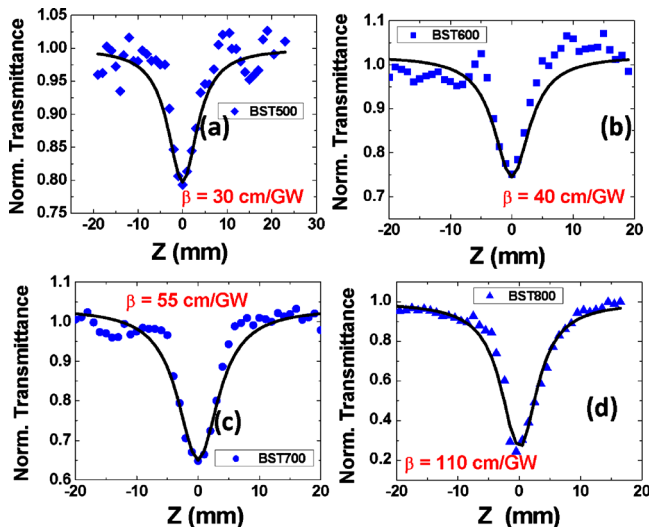


FIG. 2. (Color online) Open aperture Z-scan data with ~ 6 ns pulses (a) BST500, (b) Bst600, (c) BST700, and (d) BST800. Solid lines are the fits to experimental data. Peak intensities used were $\sim 2 \times 10^8$ W/cm 2 .

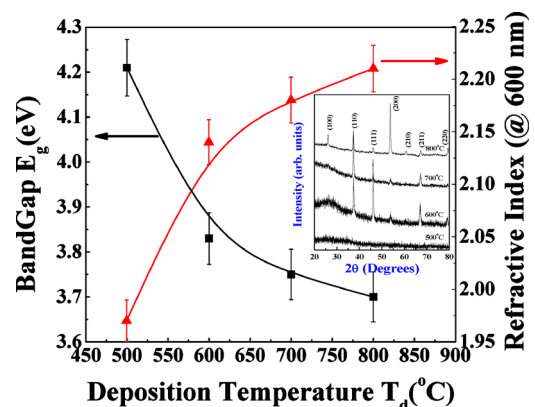


FIG. 3. (Color online) Band gap vs T_d (squares) and refractive index vs T_d (triangles). Inset shows the XRD spectra of BST films deposited at different temperatures. Solid lines are guide to the eye.

TABLE I. Summary of the nonlinear coefficients and figures of merit estimated in Ba_{0.5}Sr_{0.5}TiO₃ films.

T _d (°C)	~25 ps data			~2 ps data			~6 ns data
	n ₂ (×10 ⁻¹⁴ cm ² /W)	β (cm/W)	Figure of merit	n ₂ (×10 ⁻¹⁴ cm ² /W)	β (cm/W)	Figure of merit	β (cm/W)
500	0.11	0.16	...	0.18	0.16	T~13	30
600	0.44	0.3	T~6	40
700	2.00	α ₃ (cm ³ /W ²) 40×10 ⁻²²	W~4.9 V~0.5	0.70	α ₃ (cm ³ /W ²) 15×10 ⁻²²	V~0.57	β (cm/W) 55
800	3.25	60×10 ⁻²²	W~8.0 V~0.53	1.00	85×10 ⁻²²	V~2.3	110

The photon energy corresponding to 800 nm wavelength is 1.55 eV while the band gap of the films is >3.5 eV clearly suggesting the probable nonlinear absorption mechanism has to engage at least three photons. Since BST500 and BST600 films were found to exhibit amorphous or semicrystalline nature, the presence of some trap/defect states between the conduction and valence bands is suggested. Nonlinear absorption in this case is complex, which could arise from the presence of free-carriers in valence band and/or trap states leading to excited state absorption (ESA) rather than an instantaneous 3PA process.^{20,24} We believe that BST700 and BST800 films were entirely crystalline in nature with well defined band gap and hence 3PA prevailed. In the ns case photon energy at 532 nm corresponds to 2.33 eV and since the maximum band gap of films is ~4.2 eV, 2PA could be the plausible mechanism for nonlinear absorption.

Figures of merit²⁵ calculated from these nonlinear coefficients are also presented and obviously majority of them satisfy the conditions required for device applications (T>1 and V<0.68), especially the crystalline films. The values of NLO coefficients presented in Table I encompass an error of ±20% owing to the inaccuracies in peak intensity estimation (spot size at focus), fitting procedures, approximation of film parameters (thickness, absorption coefficient), etc. Wang *et al.*¹⁰ reported NLO studies in BST films grown with pulsed laser deposition technique at 800 °C using 55 ps pulses at an excitation wavelength 532 nm. They observed large saturable absorption type of nonlinearity with the magnitude of χ⁽³⁾~10⁻⁷ esu. They detected negative nonlinearity and its magnitude suggests either the possibility of thermal origin or a resonant nonlinearity. In the present case we used shorter pulses at 800 nm. The sign, magnitude, peak-valley separation in our case clearly indicates the origin to be of electronic type. Liu *et al.*¹¹ reported NLO properties of Ba_{0.6}Sr_{0.4}TiO₃ films on (001) MgO substrate near 800 nm and the n₂ values were ~10⁻¹⁴ cm²/W. However, they observed that simple nonlinear absorption coefficient was sufficient to explain the open aperture data. The differences in their data/samples compared to ours are (a) different stoichiometry used (Ba_{0.6}Sr_{0.4}TiO₃ in their case and Ba_{0.5}Sr_{0.5}TiO₃ in our case) implying that the T_c is different in each case and (b) usage of ~60 fs pulses and higher peak intensities (>10¹² W/cm²) than used in the present study. Gu *et al.*⁸ reported positive nonlinearities in polycrystalline BiFeO₃ films studied with 350 fs pulses and obtained n₂ value of 1.5×10⁻¹³ cm²/W. As expected, the nonlinear refractive index for films measured using ~2 ps pulses is lower than that obtained for ~25 ps pulses since the electronic contribution is significant in the former case.

In conclusion we have reported large nonlinearities in high-quality Ba_{0.5}Sr_{0.5}TiO₃ films obtained using ~2 and 25 ps pulses. The nonlinear refractive index magnitude was ~10⁻¹⁴ cm²/W while the 3PA coefficient was ~10⁻²¹ cm³/W².

Facilities provided by ACRHEM, DST, and UGC are gratefully acknowledged. We are thankful to Professor D. N. Rao and M. B. Krishna for their support in the ns Z-scan experiments.

- ¹O. Auciello, J. F. Scott, and R. Ramesh, *Phys. Today* **51**(7), 22 (1998).
- ²R. A. York, A. S. Nagra, P. Periaswamy, O. Auciello, and S. K. Streiffer, *Integr. Ferroelectr.* **34**, 1617 (2001).
- ³S. B. Majumder, M. Jain, A. Martinez, R. S. Katiyar, F. W. Van Keuls, and F. A. Miranda, *J. Appl. Phys.* **90**, 896 (2001).
- ⁴K. Venkata Saravanan, M. Ghanashyam Krishna, and K. C. James Raju, *J. Appl. Phys.* **106**, 114102 (2009).
- ⁵E. D. Mishina, N. E. Sherstyuk, V. I. Stadnichuk, A. S. Sigov, V. M. Mukhorotov, Yu. I. Golovko, A. van Etteger, and Th. Rasing, *Appl. Phys. Lett.* **83**, 2402 (2003).
- ⁶D. Y. Wang, K. P. Lor, K. K. Chung, H. P. Chan, K. S. Chiang, H. L. W. Chan, and C. L. Choy, *Thin Solid Films* **510**, 329 (2006).
- ⁷D. Y. Wang, J. Wang, H. L. W. Chan, and C. L. Choy, *Integr. Ferroelectr.* **88**, 12 (2007).
- ⁸B. Gu, Y. Wang, J. Wang, and W. Ji, *Opt. Express* **17**, 10970 (2009).
- ⁹E. D. Mishina, *Ferroelectrics* **314**, 57 (2005).
- ¹⁰W. Wang, Z. Dai, Y. Sun, Y. Sun, and D. Guan, *Appl. Surf. Sci.* **250**, 268 (2005).
- ¹¹S. W. Liu, J. Xu, D. Guzun, G. J. Salamo, C. L. Chen, Y. Lin, and M. Xiao, *Appl. Phys. B: Lasers Opt.* **82**, 443 (2006).
- ¹²P. Shi, X. Yao, L. Zhang, X. Wu, M. Wang, and X. Wan, *Solid State Commun.* **134**, 589 (2005).
- ¹³R. Reshmi, R. Sreeja, M. K. Jayaraj, J. James, and M. T. Sebastian, *Appl. Phys. B: Lasers Opt.* **96**, 433 (2009).
- ¹⁴C. Chen, T. Ning, Y. Zhou, D. Zhang, P. Wang, H. Ming, and G. Yang, *J. Phys. D: Appl. Phys.* **41**, 225301 (2008).
- ¹⁵J.-S. Kim, K.-S. Lee, and S. S. Kim, *Thin Solid Films* **515**, 2332 (2006).
- ¹⁶K.-S. Lee, I.-H. Kim, B. Cheong, W.-M. Kim, S.-H. Yoon, K.-M. Cho, H.-S. Jun, and D.-S. Kim, *Int. J. Nanosci.* **4**, 803 (2005).
- ¹⁷R. A. Ganeev, M. Suzuki, M. Baba, M. Ichihara, and H. Kuroda, *J. Opt. Soc. Am. B* **25**, 325 (2008).
- ¹⁸G. S. He, L.-S. Tan, Q. Zheng, and P. N. Prasad, *Chem. Rev.* **108**, 1245 (2008).
- ¹⁹M. Sheik-Bahae, A. A. Said, T. H. Wei, D. J. Hagan, and E. W. Van Stryland, *IEEE J. Quantum Electron.* **26**, 760 (1990).
- ²⁰R. S. S. Kumar, S. Venugopal Rao, L. Giribabu, and D. Narayana Rao, *Chem. Phys. Lett.* **447**, 274 (2007).
- ²¹R. Swanepoel, *J Phys. E* **16**, 1214 (1983).
- ²²W. A. Rachinger, *J. Sci. Instrum.* **25**, 254 (1948).
- ²³Y. G. Yang, X. W. Zhou, R. A. Johnson, and H. N. G. Wadley, *Acta Mater.* **49**, 3321 (2001).
- ²⁴B. Gu, W. Ji, X.-Q. Huang, P. S. Patil, and S. M. Dharmaparakash, *J. Appl. Phys.* **106**, 033511 (2009).
- ²⁵R. S. S. Kumar, S. Venugopal Rao, L. Giribabu, and D. Narayana Rao, *Opt. Mater. (Amsterdam, Neth.)* **31**, 1042 (2009).